China Geology 7 (2024) 642−652

China Geology

Journal homepage: http://chinageology.cgs.cn
https://www.sciencedirect.com/journal/china-geology

Hydrochemistry of the lakes in the southern Badain Jaran Desert and its paleosalinity reconstruction

Gao-lei Jiang[a, c, d], Zhe Wang[b, a,*], Zhen-long Nie[a], Zhong-shuang Cheng[a], Pu-cheng Zhu[a], Le Cao[a], Jian-mei Shen[a,*]

[a] *Institute of Hydrogeology and Environmental Geology*, *Chinese Academy of Geological Sciences*, *Shijiazhuang* 050061, *China*
[b] *China University of Geosciences*, *Wuhan* 430074, *China*
[c] *Key Laboratory of Quaternary Chronology and Hydro-Environmental Evolution*, *China Geological Survey*, *Shijiazhuang* 050061, *China*
[d] *Centre for Glacier and Desert Research*, *College of Earth and Environmental Sciences*, *Lanzhou University*, *Lanzhou* 730000, *China*

A R T I C L E I N F O

Article history:
Received 21 June 2022
Received in revised form 26 May 2023
Accepted 16 July 2023
Available online 7 September 2023

Keywords:
Mg/Ca and Sr/Ca ratios
Partition coefficient
Lake evolution
Paleoenvironmental reconstruction
Paleosalinity
Hydrochemistry
Badain Jaran Desert
Hydrogeology survey engineering

A B S T R A C T

The reconstruction of paleohydrology, especially paleosalinity, is an important component of paleoenvironmental research. Researches on the modern characteristics of lake water chemistry and the relationship between lake salinity and hydrochemistry are the basis of paleoenvironment reconstruction. The modern hydrochemical characteristics and the relationship between ion composition and salinity of modern lakes are the basis of paleosalinity reconstruction. In this study, hydrochemical analysis of 21 lakes in the Badain Jaran Desert (BJD) was carried out. The relationships between the Sr/Ca and Mg/Ca ratios and total dissolved solids (TDS) were analyzed. The results show that Na^+, K^+, Cl^- and SO_4^{2-} have high positive correlations with TDS, and Mg^{2+}, Sr^{2+}, CO_3^{2-} and HCO_3^- have lower correlations with TDS. The Sr/Ca and Mg/Ca ratios do not increase linearly with TDS. Hydrochemical analysis indicates that the studied lakes are in the carbonate precipitation stage and that evaporation is the main factor controlling lake evolution in the BJD. The relationships between the Mg/Ca and Sr/Ca ratios and TDS are mainly influenced by lake evolution stage and the hydrochemical types of the lakes. On the basis of comprehensive previous studies, the factors affecting lake evolution, the Mg and Sr partition coefficients and other hydrochemical parameters that change with lake evolution all affect the relationship between chemical composition and salinity. To reconstruct paleosalinity more accurately, more detailed research on the modern hydrochemical characteristics of lakes and the relationship between the element ratios of carbonates and water salinity should be carried out.

1. Introduction

Paleohydrological information (ion composition, ion ratio and salinity and so on) about lakes can reflect lake evolution and regional climate change and is an important component of paleoenvironmental reconstruction (Abbott MB et al., 2003; Zhai DY et al., 2011; Gouramanis C et al., 2010; Fan JW et al., 2018； McCormack J et al., 2019; Hu HP et al., 2021). The change in paleosalinity of lakes is often used as a proxy index for paleoclimate or paleoenvironmental reconstruction, which can reflect regional precipitation, evaporation information and historical lake water-level fluctuations (Shen J et al., 2000; Zhang EL et al., 2004; Curry B et al., 2016). Over several decades, many quantitative reconstruction methods of lake paleosalinity have been studied, including the transformation function between biological assemblage and lake salinity (Michelson AV et al., 2017; Mischke S et al., 2007, 2010; Zhang EL et al., 2007), the transformation function between biomarkers and lake salinity (Kou Q et al., 2022; Huang Y et al., 2021; Turich C et al., 2011), the relationship between geochemical records in carbonate and lake salinity (Sampei Y et al., 2005; Jiang GL et al., 2020; Zhang HS et al., 2023; Zhang EL et al., 2004), and the relationship between morphological character of ostracod shells (microfossils) and lake salinity (McCormack J et al.,

First author: *E-mail address*: jianggl198899@163.com (Gao-lei Jiang).

* Corresponding author: *E-mail address*: wangzhe@mail.cgs.gov.cn (Zhe Wang); sjmiheg@163.com (Jian-mei Shen).

Literary editor: Xi-jie Chen
doi:10.31035/cg2023057
2096-5192/© 2024 China Geology Editorial Office.

2019; Xu XN et al., 2012).

Among the above methods for paleosalinity reconstruction, the Mg/Ca and Sr/Ca ratios of authigenic carbonates or fossils in lake sediments are some of most commonly used qualitative or quantitative indicators to reconstruct paleosalinity (Curry B et al., 2016; McCormack J et al., 2019; Yang et al., 2014; Zhai DY et al., 2011; Zhang JW et al., 2009). This method has the following advantages: first, authigenic carbonates or fossils of carbonate composition can instantly record the hydrological information of the formation period (Engstrom DR et al., 1991; Zhang JW et al., 2009); second, minerals and fossils are generally stable after formation and can be preserved in sediment for a long time (Jiang GL et al., 2020). The idea of reconstructing paleosalinity from trace elements in carbonate or carbonate fossils has been proposed since the middle of the last century (Rucker JB et al., 1961; Odum HT, 1951; Dodd JR, 1965). When using this method to reconstruct paleosalinity, it is necessary to establish the relationship between the Sr/Ca and Mg/Ca ratios and the salinity of lake water. Then, the lake paleosalinity is reconstructed quantitatively by using the ratios of trace elements (Sr/Ca or Mg/Ca) in authigenic carbonates or fossils in lake sediments (Williams, 1966; Chivas AR et al., 1985, 1986a, 1986b; Jiang GL et al., 2020).

In previous studies, most scholars suggested that the Sr/Ca and Mg/Ca ratios of lake water are positively correlated with salinity. The positive relation between them can be expressed as:

$$\mathrm{M/Ca} = a\mathrm{S} + b \tag{1}$$

where M is Sr^{2+} or Mg^{2+}, S is lake salinity, and a and b are constants, which can be obtained from measurements of Sr or Mg and Ca and the salinity of modern lake water (Zhang EL et al., 2004).

Based on this method and the Sr/Ca ratios of ostracod fossils in lake sediments, the paleosalinities of Qinghai Lake and Daihai Lake were reconstructed quantitatively (Zhang PX et al., 1994; Zhang EL et al., 2004; Cao TJ et al., 2002). However, the evolution of lakes is a complex process. Salinity is affected not only by regional precipitation, runoff recharge but also by the concentration of some ions in lake water, lake evolution processes and other factors (Wang HL et al., 2010). The relationship between water chemical parameters or element ratios and the salinity of lake water varies at different stages of lake evolution (Ito E et al., 2009). For example, in a closed lake, the concentrations of various ions in the lake present different trends with changes in salinity. When the salinity is low, each ion increases with increasing salinity; when the salinity is high, some ions do not increase with increasing salinity, while some ions decrease with increasing salinity (Eugster HP et al., 1979; Ito E et a., 2009).

It is essential to investigate the modern characteristics of lake water chemistry to determine the relationship between lake salinity and water chemistry to reconstruct paleoenvironmental information more accurately. In this study, 21 lakes with salinities ranging from 0 g/L to 22 g/L on the southern margin of the Badain Jaran Desert (BJD) were investigated, and their ion compositions and hydrochemical characteristics were analyzed. This study provides basic hydrochemical information on lakes in the BJD and suggests caution in using ion ratios to reconstruct the paleoenvironment.

2. Geological background

The BJD is located on the northwestern Alxa Plateau in north-central China. The BJD is the second largest desert in China (5.2×10^4 km^2) and has an elevation of 900–1800 m a.s.l., falling from the southeast to the northwest (Fig. 1a; Zhu JF et al., 2010). To the south, it is bounded by the Beida Mountains and Heishantou Mountains (maximum elevation 1963 m a.s.l.), which separate it from the gobis of the Hexi Corridor (Dong ZB et al., 2013). To the southeast, it is bounded by the Yabrai Mountains (maximum elevation 1957 m a.s.l.), which separate it from the Tengger Desert. To the west and northwest, it stretches down to Ugrian Lake and the Heihe River. To the north, it is bounded by Guaizi Lake, close to the Mongolian Gobi (Dong ZB et al., 2013). The groundwater levels range from 1200 m to 800 m a.s.l. as the surface elevation descends from the southeast to the northwest (Wang Z et al., 2021; Zhang XL et al., 2021). The BJD is characterized by the coexistence of more than 110 perennial lakes and thousands of mega-dunes. The lakes lying among mega-dunes are concentrated within an area of approximately 4000 km^2 (Dong ZB et al., 2013; Wang Z et al., 2024). Most lakes are less than 0.6 km^2, and the largest is 1.46 km^2. Water depth is generally a few meters to 10 m, and the deepest lake depth is 15.9 m (Wu Y et al., 2014; Wang NA et al., 2016).

The hydrological properties of the lakes vary greatly, with the TDS values ranging from less than 1 g/L to more than 400 g/L (Lu Y et al., 2010; Yang XP et al., 2003). There is no surface runoff in the desert hinterland, and the lakes are mainly recharged by groundwater (Chen JS et al., 2004; Dong CY et al., 2016; Wang NA et al., 2016). The groundwater level around the lakes is relatively shallow, generally a few meters. The TDS values of spring water and groundwater are generally less than 1 g/L (Chen L et al., 2012). Lake water is discharged mainly through evaporation, and the annual evaporation of the lakes is approximately 1500 mm (Hu WF et al., 2015; Sun J et al., 2018; Wang LJ et al., 2024). With increasing salinity from the southeast edge to the hinterland, most lakes are the sulfate-carbonate-chloride type (Jia B et al., 2021).

The BJD has an extreme continental desert climate according to Köppe's climate classification (Dong ZB et al., 2004). The desert has an annual precipitation of 40–120 mm, descending from the southeast to the northwest. Most of the precipitation occurs in summer (Fig. 2). The potential lake surface evaporation is about 1500 mm/yr, increasing from south to north based on different studies, which is 20–30 times the amount of precipitation (Hu WF et al., 2015). The mean annual air temperature ranges from 9.5°C to 10.3°C,

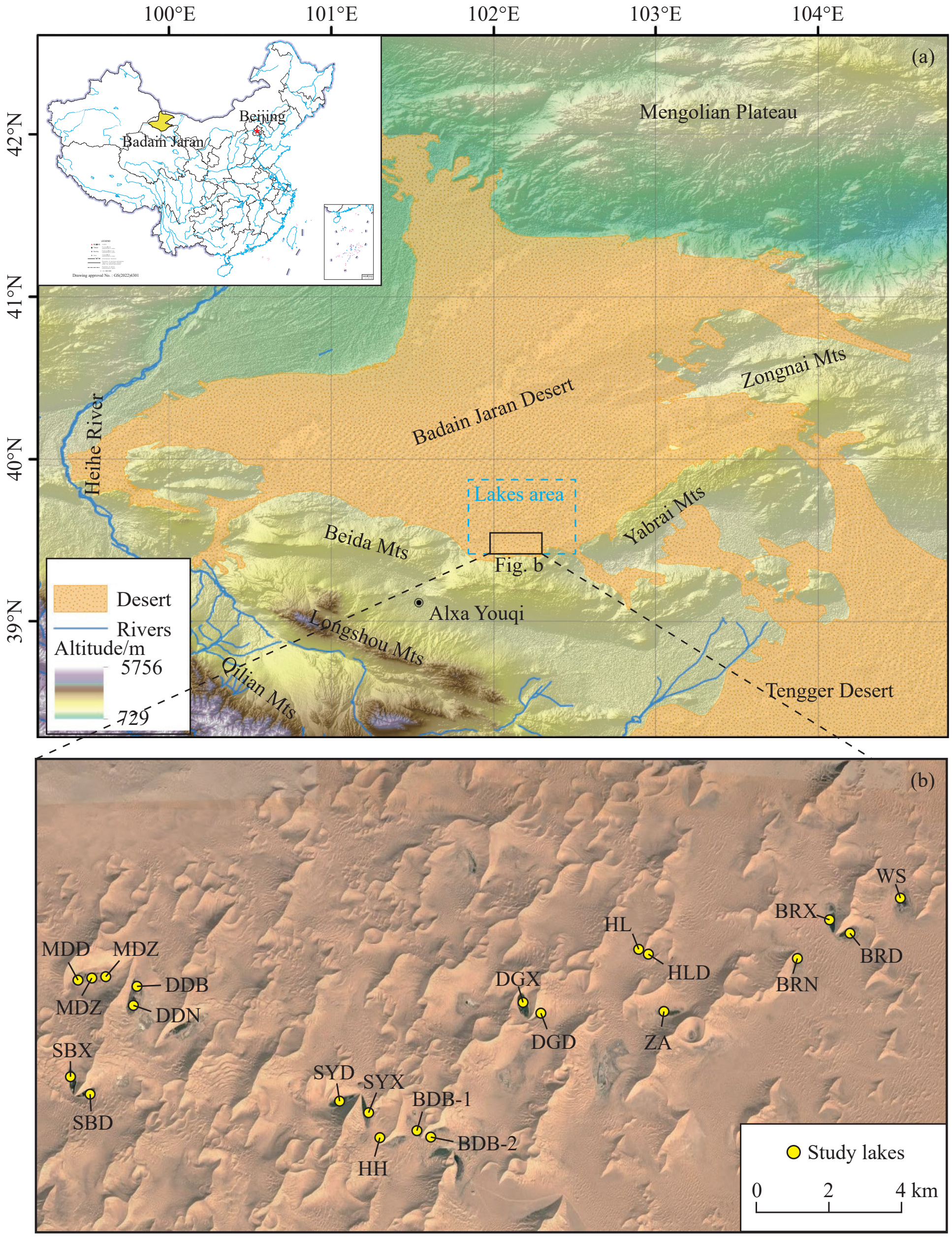

Fig. 1. Map of the Badain Jaran Desert (a) and the study lakes (b). Abbreviations: WS–Wosigetu Lake; BRD–East Baoritaolegai Lake; BRX–West Baoritaolegai Lake; BRN–South Baoritaolegai Lake; ZA–Zhasigetu Lake; HLD–East Hulusitai Lake; HL–Hulusita Lake; DGD–East Duguijaran Lake; DGX–West Duguijaran Lake; BDB-1–North Badaianjaran Lake-1; BDB-2–North Badaianjaran Lake-2; HH–Huhewuzhuer Lake; SYD–East Sayinwusu Lake; SYX–West Sayinwusu Lake; SBD–East Shaobaijaran Lake; SBX–West Shaobaijaran Lake; DDN–South Dundejaran Lake; DDB–North Dundejaran Lake; MDD–East Modanjaran Lake; MDZ–Middle Modan Lake (MDZ); MDX–West Modanjaran Lake .

with the lowest monthly mean temperature in January and the highest in July (Fig. 2). The mean annual wind speed ranges from 2.8 m/s to 4.6 m/s, increasing from south to north, and the strongest winds occur in April and May (Dong ZB et al., 2013).

The surface vegetation coverage of the BJD is very low, ranging from 5 to 50. The vegetation is dominated by xerophytic and ultraxerophytic shrubs and subshrubs, and herbacea is dominated by annual plants. The vegetation is mainly distributed in the dry lake basin and around the lakes. The vegetation is distributed in belts around the lake shores, with areal extents of tens of metres. Due to the high salinity, there are no fish in the lakes, and few animals drink the lake water. There are only a few herders living around a few lakes.

3. Samples and methods

Twenty-one lakes were investigated, and water samples were collected in September 2017. The sample sites are shown in Fig. 1b. The sampling sites were generally 1–6 m away from the lake shore, and the water depth ranged from 0.5 m to 1.5 m. TDS and salinity information was measured by using a hand-held water quality analyzer (MULTI 3400). Water samples were collected in 500 ml polyethylene bottles, which were moistened and washed 3 times before sample

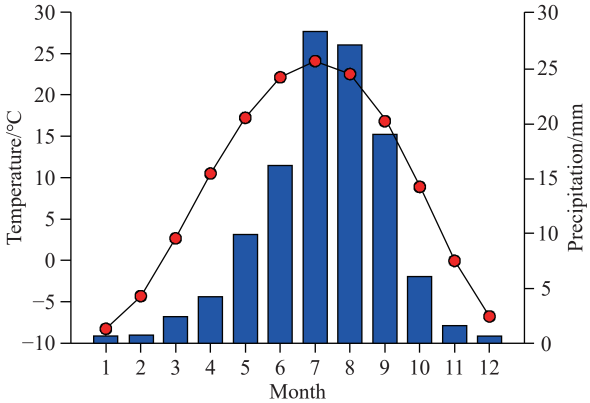

Fig. 2. Monthly mean temperature and precipitation of the Badain Jaran Desert during 1960–2018.

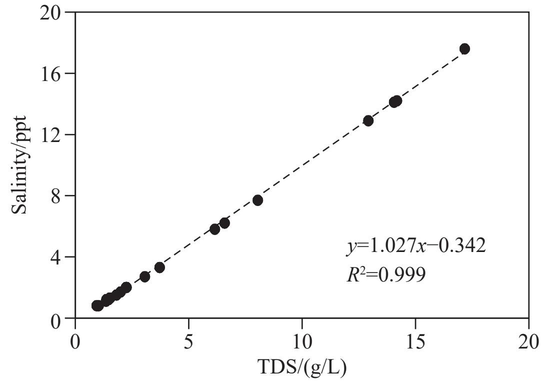

Fig. 3. Relationship between TDS and salinity using hand-held water quality analyzer.

collection. Water samples were kept sealed at −4°C in the laboratory for analysis. The cations (K^+, Na^+, Ca^{2+}, Mg^{2+}, Sr^{2+}) were analyzed by inductively coupled plasma spectrometer (Optima 8000). $Cl^−$, $SO_4^{2−}$ were analyzed by ion chromatograph (ICS-1500), $HCO_3^−$, $CO_3^{2−}$ were analyzed by using titration. TDS was measured by electronic scales. The above analytical tests are done at the Groundwater Mineral Water and Environmental Monitoring Center of the Institute of Hydrogeology and Environmental Geology, Chinese Academy of Geological Sciences. The test environment temperature was 23°C, and the humidity was 48%. The reliability of the hydrochemical data was assessed by checking ion balances. Ion charge imbalances were within ± 5%.

In this study, the Shukalev classification method was adopted for the calculation of hydrochemical types. Ions greater than 5% but less than 25% are in brackets; ions greater than 25% are indicated in order of abundance (Wang DC et al., 1980). The saturation index was calculated by using AquaChem 4.0 Software.

4. Results and discussion

4.1. Hydrochemical characteristics of lake water

The results of hand-held water quality analyzer show that salinity has a good linear relationship with TDS (Fig. 3). Therefore, the relationship between each parameter and TDS is discussed using laboratory data. The laboratory analysis results are shown in Table 1. The results show that the TDS of the collected lake samples ranges from 0.970 g/L to 22.221 g/L. The order of cation concentrations in the lakes is Na^+> Mg^{2+}>Ca^{2+} and K^+, and the order of anion concentrations is $Cl^−$>$SO_4^{2−}$>$HCO_3^−$>$CO_3^{2−}$. The Piper trigram shows that Na^+ is predominant in all the lake samples, with ion concentrations of up to 6.898 g/L in SYD Lake (Fig. 4). There is little Ca^{2+} and Mg^{2+} in the lakes with lower salinity (Fig. 4). Anion trigonometry shows that $Cl^−$ is the most abundant in all lakes, followed by $SO_4^{2−}$, and a few lakes contain $CO_3^{2−}$ and $SO_4^{2−}$. According to calculations, the water chemistry types of the collected water samples are mainly Na-Cl-SO_4, Na-Cl and Na-Cl-HCO_3, which is basically consistent with the water chemistry results from Lu Y et al. (2010) and Chen L et al. (2012), indicating that the water chemistry of lakes in the BJD is relatively stable.

Fig. 5 shows that the main ions except Ca^{2+} increase with increasing TDS. Na^+, K^+, $Cl^−$ and $SO_4^{2−}$ have high correlations with TDS, and Mg^{2+}, Sr^{2+}, $CO_3^{2−}$ and $HCO_3^−$ have lower correlations with TDS (Fig. 5). When TDS is low, the Ca^{2+} content is dispersed, and some lakes have higher Ca^{2+} contents than average (0.016 g/L). With increasing TDS, the Ca^{2+} content shows a weak upward trend (Fig. 5d). The Sr/Ca ratio ranges from 0.005 to 0.221, and the Mg/Ca ratio ranges from 1.916 to 102.692. Fig. 6 shows that the Sr/Ca and Mg/Ca ratios of lake water do not increase linearly with increasing TDS. The Sr/Ca ratio decreases with increasing TDS when the TDS is below 4.0 g/L (Fig. 6a).

4.2. Lake evolution stage

The evolution of lake water is influenced by many factors, such as evaporation, precipitation, water-rock reactions and runoff recharge (Hardie LA et al., 1970; Chen J et al., 2021; Kolpakova MN et al., 2019; Yu LS et al., 2021). For the lakes in the BJD, there is no runoff recharge. The origin of recharge sources remains a hotly debated issue, and there are mainly the following viewpoints: (1) rainfall and/or snow meltwater from the Qilian Mountains or the Qinghai-Tibet Plateau recharge desert groundwater through deep faults (Chen JS et al., 2004); (2) lakes in the desert areas are mainly recharged by surface runoff and groundwater caused by meteoric water from local or surrounding mountainous areas (Liu CK et al., 2016; Jiang GL et al., 2021a); and (3) precipitation formed under cold (glacial) environments during the late Pleistocene in the mountainous area on the southeastern margin of the desert is the main recharge source of groundwater in the lake area (Gates JB et al., 2008a, b). Although the recharge source of desert groundwater is much debated, the lakes in the desert are recharged by local groundwater. Modern observations suggest that the replenishment of lakes by local precipitation is limited (Ma N et al., 2014). Water balance calculation results suggest that more than 90% of the recharge of lakes between megadunes is from groundwater in the BJD (Dong

Table 1. Hydrochemical indicators of water samples from lakes in the BJD.

Lakes	K^+/(g/L)	Na^+/(g/L)	Ca^{2+}/(g/L)	Mg^{2+}/(g/L)	Sr^{2+}/(g/L)*	HCO_3^-/(g/L)	CO_3^{2-}/(g/L)	Cl^-/(g/L)	SO_4^{2-}/(g/L)	TDS/(g/L)
BRN	0.030	0.387	0.046	0.046	0.0004	0.190	0.029	0.466	0.316	1.387
BRX	0.037	0.368	0.069	0.069	0.0003	0.277	0.033	0.429	0.382	1.469
BRD	0.018	0.382	0.047	0.047	0.0013	0.190	/	0.481	0.339	1.403
WS	0.015	0.264	0.034	0.034	0.0009	0.321	/	0.238	0.225	0.970
ZA	0.017	0.422	0.028	0.028	0.0008	0.355	0.029	0.341	0.324	1.357
HL	0.053	0.806	0.147	0.147	0.0003	0.629	0.047	0.849	0.867	3.108
HLD	0.020	0.322	0.062	0.062	0.0013	0.421	/	0.392	0.243	1.299
DGX	0.013	0.727	0.017	0.017	0.0008	0.412	0.029	0.606	0.553	2.168
DGD	0.048	0.582	0.054	0.054	0.0010	0.681	0.163	0.497	0.306	2.001
BDB	0.145	2.046	0.235	0.235	0.0040	0.711	0.373	2.556	1.504	7.231
BDBB	0.310	4.342	0.534	0.534	0.0055	1.006	0.361	5.357	3.358	14.791
HH	0.336	5.175	0.397	0.397	0.0001	1.853	0.600	5.515	4.041	17.011
SBD	0.039	0.475	0.086	0.086	0.0003	0.507	0.041	0.515	0.324	1.757
SBX	0.038	0.602	0.104	0.104	0.0003	0.252	0.035	0.765	0.474	2.164
MDX	0.039	0.443	0.063	0.063	0.0004	0.319	0.111	0.415	0.311	1.554
MDZ	0.102	1.263	0.085	0.085	0.0013	0.836	0.432	0.902	0.924	4.139
MDD	0.224	2.954	0.105	0.105	0.0015	1.581	0.551	2.538	1.775	8.959
DDB	0.154	2.117	0.105	0.105	0.0012	1.197	0.542	1.970	1.169	6.668
DDN	0.027	0.266	0.026	0.026	0.0005	0.362	0.023	0.182	0.186	0.907
SYX	0.320	4.614	0.552	0.552	0.0088	1.143	0.472	6.040	3.606	16.207
SYD	0.393	6.898	0.563	0.563	0.0066	1.380	0.542	7.265	5.838	22.221

Note: *Sr^{2+} content retains four decimal places.

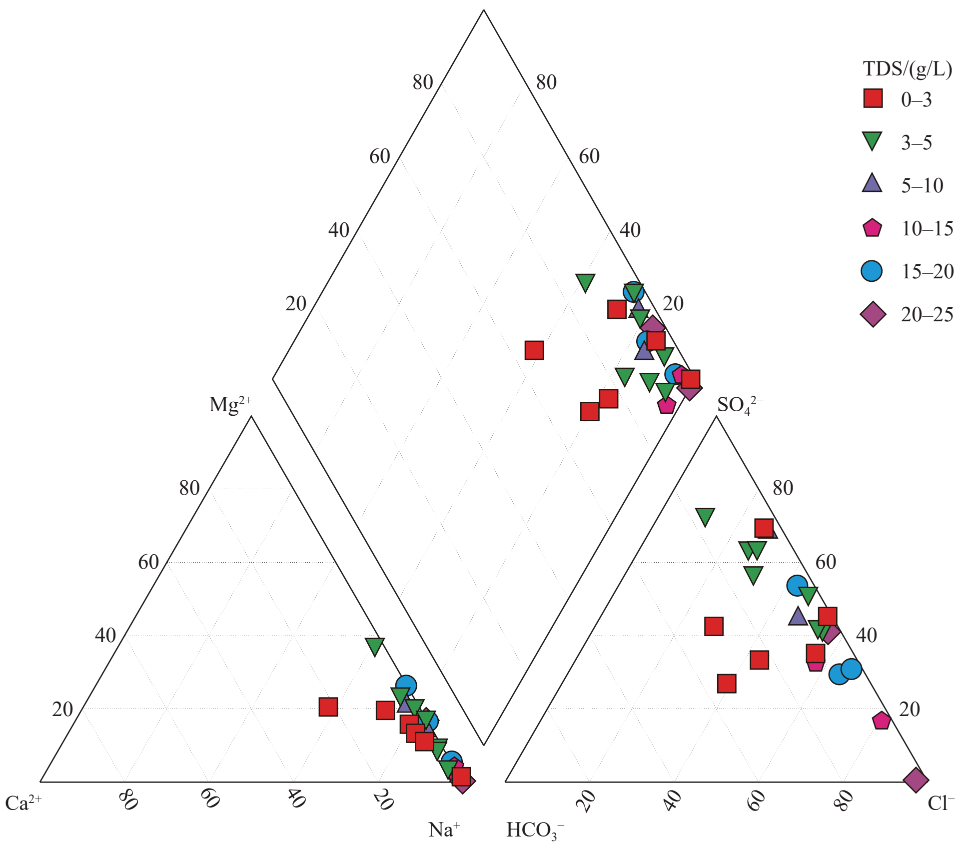

Fig. 4. Piper diagram of the chemical composition of the lakes in the southern BJD.

CY et al., 2016; Wang NA et al., 2016).

Gibbs plots show that the TDSs of lakes in the BJD are affected by evaporation (Fig. 7). In arid regions, evaporation is more important than precipitation for lake evolution (Song SH et al., 2023; Wu D et al., 2020; Yu C et al., 2022). Based on eddy correlation system observations, lake evaporation calculations show that the average evaporation is 3.97 mm/d and the cumulative evaporation is 1450±10 mm, which

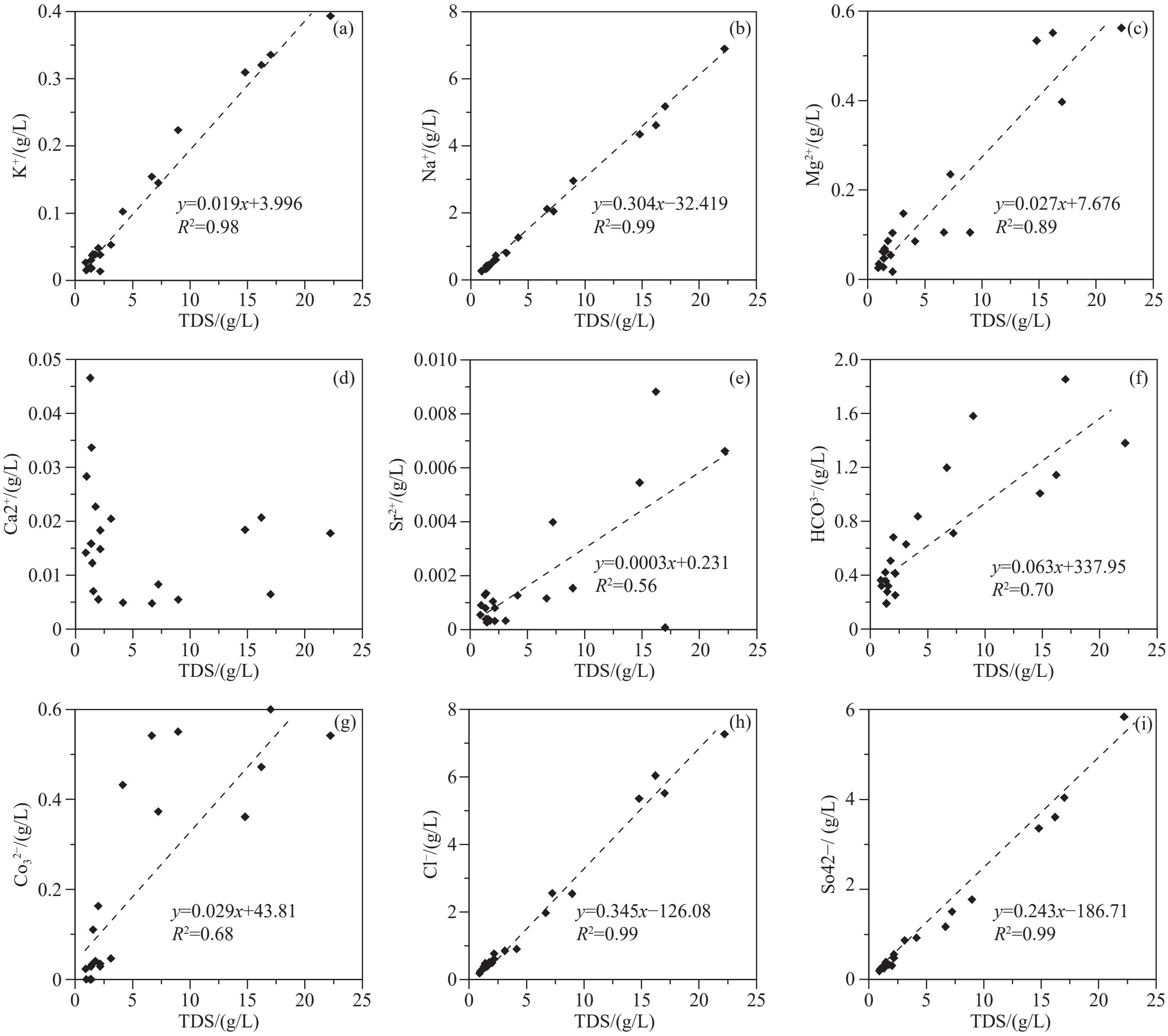

Fig. 5. Relationship between different ion contents and TDS.

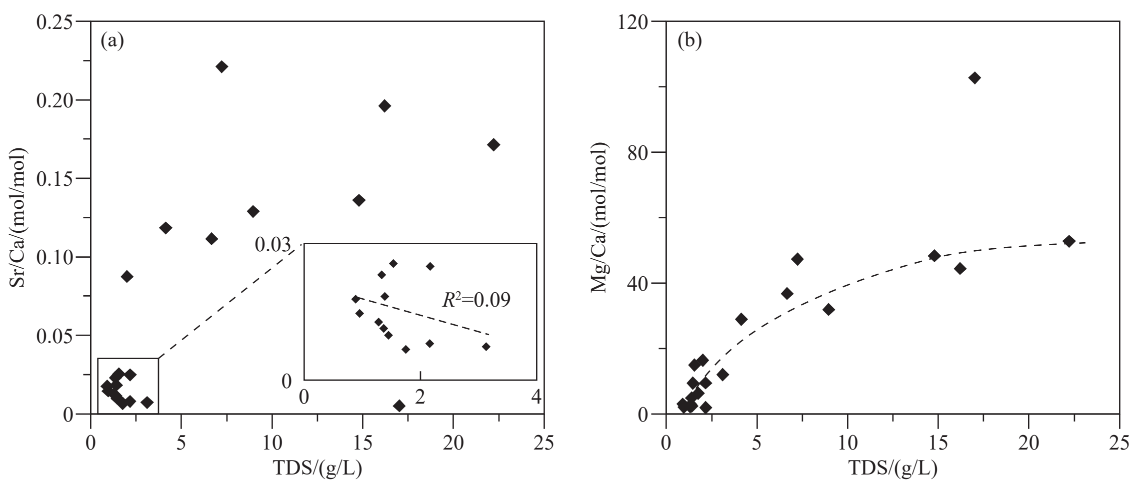

Fig. 6. Relationship between Sr/Ca (a) and Mg/Ca (b) ratios and TDS.

exceed the cumulative precipitation by 20-fold during the same period (Hu WF et al., 2015). Modern observational data show that the annual evaporation is 1500 mm in the BJD, and lake evaporation is mainly affected by temperature (Han PF et al., 2018). The lake evolution over the past 140 years also indicates that evaporation is the main factor affecting the evolution, and rises in temperature can enhance evaporation and then the salinization of lake water and carbonate precipitation (Jiang GL et al., 2021b). The lakes in the desert area have a warm island effect, resulting in the surface temperature of the lakes being approximately 1.6°C higher than that in the desert area, which can enhance the evaporation effect (Liang XY et al., 2020). In the BJD, there is no other drainage path for lakes except evaporation. The TDS of groundwater in the BJD is low, with most values below 1 g/L (Cao L et al., 2017; Chen L et al., 2012). The high salinity of most lakes in the BJD also indicates that evaporation has an important effect on the lakes.

As evaporation proceeds, ions accumulate in the lake and form salt minerals. Based on the Harde & Eugster theory, the precipitation of minerals follows a chemical divide according to the order carbonate, sulfate and chloride (Hardie LA et al., 1970). This theory allows us to determine the stage of a lake's evolution (Kolpakova MN et al., 2019; Liu XQ, 2008). According to the model, the studied lakes are in the stage of Ca and HCO_3 removal (Fig. 8a) and have not yet reached the stages of sulfate precipitation (Fig. 7a). The saturation index values of dolomite, calcite and aragonite are greater than 0, while the saturation index values of gypsum and rock salt are below 0, indicating that the lake is in the stage of carbonate deposition (in particular, the average saturation index of dolomite is 3) (Fig. 9). The mineral composition of lake sediments in the BJD showed that the salt minerals are mainly carbonate in the lakes with a salinity of several grams per liter or tens of grams per liter, which also indicates that the lakes are in the stage of carbonate precipitation (Ma SH et al., 2015).

4.3. Implication for paleosalinity reconstruction

The Mg/Ca and Sr/Ca ratios of authigenic carbonates or fossils in lake sediments are commonly used as indicators to reconstruct paleosalinity (Shen J et al., 2000; Zhang EL et al., 2004; Hu HP et al., 2021). However, this study indicates that the Mg/Ca and Sr/Ca ratios do not always have a linear positive relationship with salinity. Although the Mg/Ca ratio increases with the increasing TDS, the increase is not linear in this study. And, the relationship between Mg/Ca ratio and TDS is more complex. The hydrochemical characteristics and saturation index indicate that the lakes are in the stage of carbonate precipitation (Fig. 8; Fig. 9). When carbonate

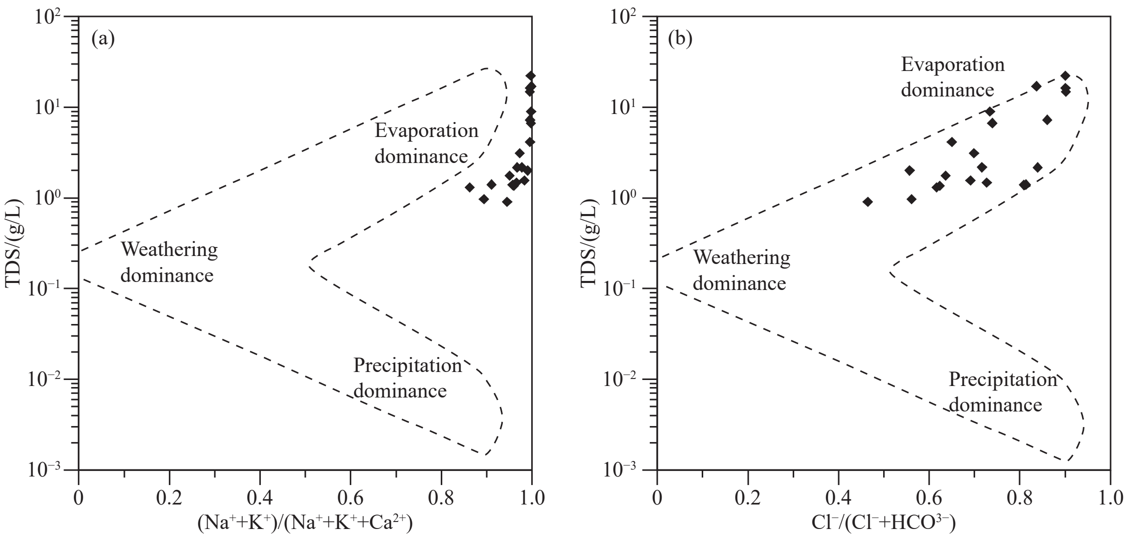

Fig. 7. Gibbs plots indicating dominant processes for the formation of lake water.

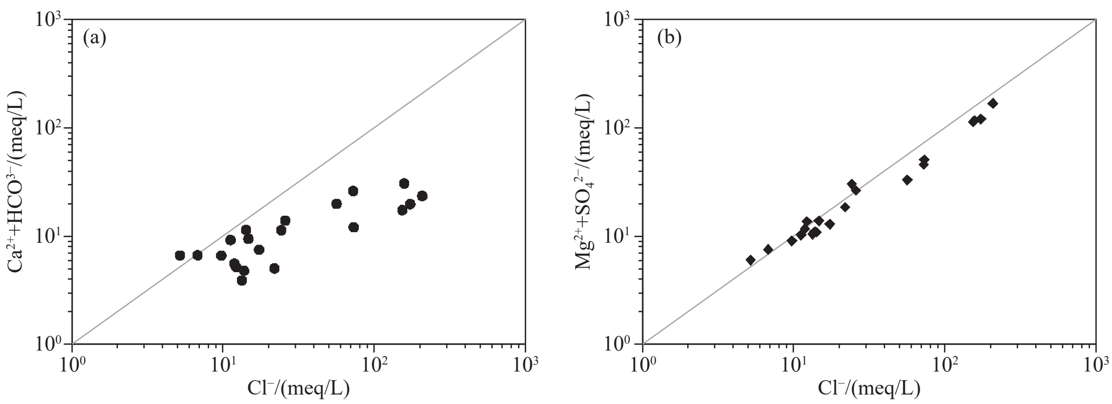

Fig. 8. Ca^{2+} and HCO_3^- (a) and Mg^{2+} and SO_4^{2-} (b) as a function of Cl^- content in lake water. The solid line corresponds to the positions of points expected by simple evaporation (Hardie LA et al., 1970).

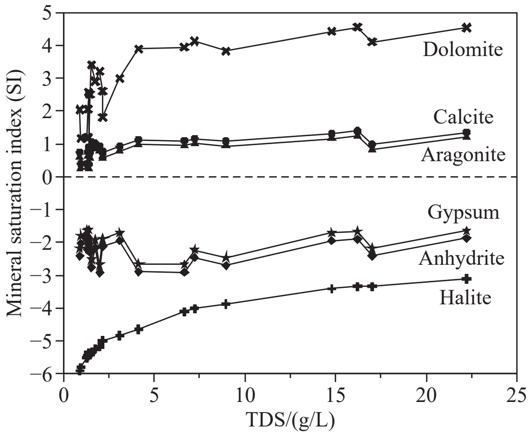

Fig. 9. Saturation index of minerals in the lakes of the study area.

precipitation occurs, Ca^{2+}, HCO_3^-, and minor to trace amounts of Mg^{2+} and Sr^{2+} are removed from the water as endogenic carbonates, which changes the relationship between ions (Ca^{2+}, Mg^{2+}, Sr^{2+} and HCO_3^-) and TDS (Ito E et al., 2009). Moreover, differences in carbonates affect the contents of different ions or ion ratios. For example, because the ions Sr and Ca have similar ionic radii and often enter mineral crystals by isomorphic substitution to replace Ca, when aragonite deposits occur in a lake, the content of Sr in the water will also rapidly decrease. Therefore, when there are carbonate deposits in a lake, the Mg/Ca and Sr/Ca ratios of the lake water tend to decrease.

The relationship between water Mg/Ca ratio and salinity becomes more complex with lake evolution stage changes. For some salt lakes in the Qinghai-Tibet Plateau, there is even a significant negative correlation between Ca and salinity in the process of brine evaporation (Wang HL et al., 2010). With the concentration or dilution of lake water, the correlation between lake salinity and Mg^{2+} becomes extremely high, but the correlation between salinity and Ca^{2+} is very unstable (Wang HL et al., 2010). For lakes of the same hydrochemical type, the correlation between Mg^{2+} and salinity is weak in the carbonate stage, strong in the sulfuric acid stage and strongest in the chloride stage (Wang HL et al., 2010). In the lake water evolutionary pathway toward calcium depletion, the Mg/Ca ratio has a positive relationship with the TDS of lakes in western Mongolia (Van der Meeren T et al., 2011). Ion concentrations and the relationship between the Mg/Ca and Sr/Ca ratios and salinity are complex, such as in lakes with Alk >Ca.

For quantitative reconstruction of paleolake salinity, factors affecting lake evolution and the establishment of quantitative relationships also need to be considered. First, the main factors affecting lake evolution, especially precipitation and evaporation, may change during the long evolution history (Li ZL et al., 2016; Wu D et al., 2020). Second, the Mg and Sr partition coefficients between carbonate or fossils and lake water are important. However, the partition coefficient is not a constant and is also affected by lake evolution and other factors (Jiang GL et al., 2020). Third, during the stable lake evolution stage, other ion contents or hydrochemical parameters other than salinity changes (i.e., alkalinity, CO_2 concentration) also affect the Sr, Mg, and Ca contents or their ratios (Eugster et al., 1979; Ito E et al., 2009; Van der Meerren T et al., 2011).

Paleosalinity reconstruction is an important component of paleoenvironmental reconstruction. In desert areas, materials that can be used to reconstruct paleoenvironments are limited. Previous studies were mostly qualitative reconstructions (Dong GR et al., 1995; Ma JZ et al., 2004; Yang XP, 2000). Carbonate deposits, or fossils of carbonate composition, which have great potential for quantitative reconstruction of the paleoenvironment, are common in desert areas (Ma SH et al., 2015; Jiang GL et al., 2020, 2022a, b; Li Z et al., 2019). More studies on the relationship between the element ratios of carbonates and water salinity should be carried out in desert areas.

5. Conclusions

(i) The studied lakes on the southern margin of the BJD have salinities ranging from 0.97 g/L to 22.22 g/L. Na^+, K^+, Cl^- and SO_4^{2-} have high positive correlations with TDS, and Mg^{2+}, Sr^{2+}, CO_3^{2-} and HCO_3^- have lower correlations with TDS. The Sr/Ca and Mg/Ca ratios do not increase linearly with TDS. The water chemistry types of the lakes are mainly Na-Cl-SO_4, Na-Cl and Na-Cl-HCO_3 and have been relatively stable in recent decades.

(ii) Hydrochemical analysis indicated that the studied lakes are in the carbonate precipitation stage and that evaporation is the main factor affecting lake evolution in the BJD. The relationship between the Mg/Ca and Sr/Ca ratios and TDS is largely influenced by lake evolution and hydrochemical type. In addition, paleosalinity reconstruction is also affected by the partition coefficients of Mg and Sr and other hydrochemical parameters of lakes. More research on modern lake hydrochemical characteristics should be carried out.

CRediT authorship contribution statement

Gao-lei Jiang conceived of the presented idea. Zhen-long Nie Zhe Wang and Jian-mei Shen developed the theory and performed the computations. Zhong-shuang Cheng, Pu-cheng Zhu and Le Cao verified the analytical methods. All authors discussed the results and contributed to the final manuscript. All authors listed have made substantial, direct, and intellectual contributions to the work and approved it for publication.

Declaration of competing interest

The authors declare no conflicts of interest.

Acknowledgments

This research was financially supported by the Basic Research Program of Chinese Academy of Geological Sciences (CAGS) (YK202302)，the projects of the China

Geological Survey (DD20221929, 121201106000150093) and the National Natural Science Foundation of China (41807420).

References

Abbott MB, Wolfe BB, Wolfe AP, Seltzer GO, Aravena R, Mark BG, Polissar PJ, Rodbell DT, Rowe HD, Vuille M. 2003. Holocene paleohydrology and glacial history of the central Andes using multiproxy lake sediment studies. Palaeogeography, Palaeoclimatology, Palaeoecology, 194, 123–138. doi: 10.1016/S0031-0182(03)00274-8.

Cao L, Nie ZL, Liu XQ, Wang Z, Meng LQ, Jiang GL. 2017. Hydrochemical cause of lakes' tufa in Badian Jaran Desert. Journal of Desert Research, 37(5), 1026–1034 (in Chinese with English abstract). doi: 10.7522/j.issn.1000-694X.2016.00101.

Cao TJ, Duan XJ, Wang SM, Shen J. 2002. An 800-year reconstruction of paleosalinity in Daihai Lake water and its implications of climate change. Earth Science Frontiers (China University of Geosciences, Beijing),9(1), 187–192 (in Chinese with English abstract). doi: 10.3321/j.issn:1005-2321.2002.01.023.

Chen J, Qian H, Gao YY, Wang HK, Zhang MS. 2021. Insights into hydrological and hydrochemical processes in response to water replenishment for lakes in arid regions. Journal of Hydrology, 581, 124386. doi: 10.1016/j.jhydrol.2019.124386.

Chen JS, Li L, Yang J, Wang S, Barry DA, Sheng XF, Gu WZ, Zhao X, Chen L. 2004. Groundwater maintains dune landscape. Nature, 432, 459–460. doi: 10.1038/432459a.

Chen L, Wang NA, Wang H, Dong CY, Lu Y, Lu JW. 2012. Spatial patterns of chemical parameters of lakes and groundwater in Badain Jaran Desert. Journal of Desert Research, 32(2), 531–538 (in Chinese with English abstract). doi: 10.1007/s11783-011-0280-z.

Chivas AR, De Deckker P, Shelley JMG. 1986a. Magnesium and strontium in non-marine ostracod shells as indicators of palaeosalinity and palaeotemperature. Hydrobiologia, 143(1), 135–142. doi: 10.1007/BF00026656.

Chivas AR, De Deckker P, Shelley JMG. 1986b. Magnesium content of non-marine ostracod shells: A new palaeosalinometer and palaeothermometer. Palaeogeography, Palaeoclimatology, Palaeoecology, 54(1), 43–61. doi: 10.1016/0031-0182(86)90117-3.

Chivas AR, De Dekker P, Shelley JMG. 1985. Strontium content of ostracods indicates lacustrine paleosalinity. Nature, 316(6025), 251–253. doi: 10.1038/316251a0.

Curry B, Henne PD, Mesquita-Joanes F, Marrone F, Pieri V, Mantia TL, Calò C, Tinner W. 2016. Holocene paleoclimate inferred from salinity histories of adjacent lakes in southwestern Sicily (Italy). Quaternary Science Reviews, 150, 67–83. doi: 10.1016/j.quascirev.2016.08.013.

Dodd JR. 1965. Environmental control of strontium and magnesium in *Mytilus*. Geochimica Et Cosmochimica Acta, 29, 385–398. doi: 10.1016/0016-7037(65)90035-9.

Dong CY, Wang NA, Chen JS, Li ZL, Chen HB, Chen L, Ma N. 2016. New observational and experimental evidence for the recharge mechanism of the lake group in the Alxa Desert, north-central China. Journal of Arid Environments, 124, 48–61. doi: 10.1016/j.jaridenv.2015.07.008.

Dong GR, Gao QZ, Zou XY, Li BS, Yan MC. 1995. Climate changes at southern fringe of the Badain Jaran desert since Pleistocene. Chinese Science Bulletin, 40(13), 423–4237. doi: 10.1007/BF02006258.

Dong ZB, Qian GQ, Lv P, Hu GY. 2013. Investigation of the sand sea with the tallest dunes on Earth: China's Badain Jaran Sand Sea. Earth Science Reviews, 120, 20–39. doi: 10.1016/j.earscirev.2013.02.003.

Dong ZB, Wang T, Wang XM. 2004. Geomorphology of the mega-dunes in the Badain Jaran Desert. Geomorphology 60 (1–2), 191–203. doi: 10.1016/j.geomorph.2003.07.023.

Engstrom DR, Nelson SR. 1991. Paleosalinity from trace in fossil ostracodes compared with observational records at Devils Lake, North Dakota, USA. Palaeogeography, Palaeoclimatology, Palaeoecology, 295–312. doi: 10.1016/0031-0182(91)90057-X.

Eugster HP, Jones BF. 1979. Behavior of major solutes during closed-basin brine evolution. American Journal of Science, 279, 609–631. doi: 10.2475/ajs.279.6.609.

Fan JW, Xiao JL, Wen RL, Zhang SR, Huang Y, Yue JJ, Wang X, Cui LL, Li H, Xue DS, Liu YH. 2018. Mineralogy and carbonate geochemistry of the Dali Lake sediments: Implications for paleohydrological changes in the East Asian summer monsoon margin during the Holocene. Quaternary International, 527, 103–112. doi: 10.1016/j.quaint.2018.03.019.

Gates JB, Edmunds WM, Darling WG, Ma JZ, Pang ZH, Young AA. 2008a, Conceptual model of recharge to southeastern Badain Jaran Desert groundwater and lakes from environmental tracers. Applied Geochemistry, 23, 3519–3534. doi: 10.1016/j.apgeochem.2008.07.019.

Gates JB, Edmunds WM, Ma JZ, Scanlon BR. 2008b. Estimating groundwater recharge in a cold desert environment in northern China using chloride. Hydrogeology Journal, 16(5), 893–910. doi: 10.1007/s10040-007-0264-z.

Gouramanis C, Wilkins D, Deckker PD. 2010. 6000 years of environmental changes recorded in Blue Lake, South Australia, based on ostracod ecology and valve chemistry. Palaeogeography, Palaeoclimatology, Palaeoecology, 297, 223–237. doi: 10.1016/j.palaeo.2010.08.005.

Han PF, Wang XS, Hu XN, Jiang XW, Zhou YY. 2018. Dynamic relationship between lake surface evaporation and meteorological factors in the Badain Jaran Desert. Arid Zone Research, 35(5), 1012–1020. doi: 10.13866/j.azr.2018.05.02.

Hardie LA, Eugster HP. 1970. The evolution of closed-basin brines. Mineralogical Society of America, Special Paper, 3, 273–290.

Hu HP, Feng JL, Liu JH, Wu XP, Chen F, Zhang JF, Pei LL, Wang KY, Ye CS. 2021. Paleo-hydrochemistry reconstructed from fossil mollusk shells from dammed paleo-lake sediments in the Yarlung Tsangpo valley, Tibet. Applied Geochemistry, 132, 105069. doi: 10.1016/j.apgeochem.2021.105069.

Hu WF, Wang NA, Zhao LQ, Ning K, Zhang HX, Sun J. 2015. Water-heat exchange over a typical lake in Badain Jaran Desert, China. Progress in Geography, 34(8), 1061–1071 (in Chinese with English abstract). doi: 10.18306/dlkxjz.2015.08.013.

Huang YS, Zheng YS, Heng P, Giosan L, Coolen MJL. 2021. Black Sea paleosalinity evolution since the last deglaciation reconstructed from alkenone-inferred Isochrysidales diversity. Earth and Planetary Science Letters, 564, 116881. doi: 10.1016/j.epsl.2021.116881.

Ito E, Forester R M. 2009. Changes in continental ostracode shell chemistry: Uncertainty of cause. Hydrobiologia, 620(1), 1–15. doi: 10.1007/s10750-008-9622-7.

Jia B, Si JH, Xi HY, Qin J. 2021. A characterization of the hydrochemistry and main controlling factors of lakes in the Badain Jaran Desert, China. Water, 13, 2931. doi: 10.3390/w13202931.

Jiang GL, Liu LJ, Mao X. 2020. Trace elements in non-marine Ostracods and their application to paleoenvironment reconstruction. Marine Geology & Quaternary Geology, 40(2), 192–199 (in Chinese with English abstract). doi: 10.16562/j.cnki.0256-1492.2019041601.

Jiang GL, Nie Z L, Liu Z, Wang Z, Zhao H, Yang JS, Shen JM. 2021a. OSL ages and its hydrological implications of alluvial-diluvial deposits from the southern margin of Badain Jaran Desert. Earth Science, 46(5), 1829–1839 (in Chinese with English abstract). doi: 10.3799/dqkx.2020.148.

Jiang GL, Wang NA, Mao X, Zhao H, Liu LJ, Shen JM, Nie ZL, Wang

Z. 2021b. Hydrological evolution of a lake recharged by groundwater in the Badian Jaran Desert over the Past 140 years. Frontiers in Earth Science, 9, 721724. doi: 10.3389/feart.2021.721724.

Jiang GL, Wang NA, Li ZL, Li M, Su XB, Ning K. 2022a. Distribution pattern of saline minerals in surface sediments from lakes in the Badain Jaran Desert and its implications for climate-environmental reconstruction. Geology in China (in Chinese with English abstract). doi: 10.12029/gc20220304004.

Jiang GL, Wang NA, Zhai DY, Li XZ, Mao X, Li M, Liu LJ. 2022b. Distribution pattern of different phenotypes of Limnocythere inopinata (an ostracod) from lakes in the Badain Jaran Desert, northern China. Ecological Indicators, 139, 108965. doi: 10.1016/j.ecolind.2022.108965.

Kolpakova MN, Gaskova OL, Naymushina OS, Karpov AV, Vladimirov AG. 2019. Saline lakes of Northern Kazakhstan: Geochemical correlations of elements and controls on their accumulation in water and bottom sediments. Applied Geochemistry, 107, 8–18. doi: 10.1016/j.apgeochem.2019.05.013.

Kou Q, Zhu LP, Ju JT, Wang JB, XU T, LI GL, Ma QF. 2022. Influence of salinity on glycerol dialkyl glycerol tetraether-based indicators in Tibetan lakes: Implications for paleotemperature and paleosalinity reconstructions. Palaeogeography, Palaeoclimatology, Palaeoecology, 601, 111127. doi: 10.1016/j.palaeo.2022.111127.

Li ZL, Chen QJ, Zhang C, Yu QJ, Dong SP, Zhao LQ, Wang NA. 2019. Environmental Significance of the Chemical Composition of Sediments in Groundwater-Recharged Lakes of the Badain Jaran Desert, NW China. Geochemistry, Geophysics, Geosystems, 20, 1026–1040. doi: 10.1029/2018GC007967.

Liang XY, Zhao LQ, Xu XB, Niu ZM, Zhang WJ, Wang NA. 2020. Plant phenological responses to the warm island effect in the lake group region of the Badain Jaran Desert, northwestern China. Ecological Informatics, 57, 101066. doi: 10.1016/j.ecoinf.2020.101066.

Liu CK, Liu J, Wang XS, Zheng CM. 2016. Analysis of groundwater-lake interaction by distributed temperature sensing in Badain Jaran Desert, Northwest China. Hydrological Processes, 30(9), 1330–1341. doi: 10.1002/hyp.10705.

Liu XQ, Dong HL, Rech JA, Matsumoto R, Yang B, Wang YB. 2008. Evolution of Chaka Salt Lake in NW China in response to climatic change during the Latest Pleistocene-Holocene. Quaternary Science Reviews, 27, 867–879. doi: 10.1016/j.quascirev.2007.12.006.

Lu Y, Wang NA, Li GP, Li ZL, Dong CY, Lu JW. 2010. Spatial distribution of lakes hydro-chemical types in Badain Jaran Desert. Journal of Lake Science, 22(5), 774–782 (in Chinese with English abstract). doi: 10.18307/2010.0521.

Ma JZ, Chen FH, Zhao H. 2004. Change on climate and groundwater recharge from geochemical records of unsaturated zone in the Badain Jaran Desert in the recent 1000 years. Chinese Science Bulletin, 49(1), 22–27. doi: 10.3321/j.issn:0023-074X.2004.01.004.

Ma N, Wang NA, Zhao LQ, Zhang ZY, Dong CY, Shen SP. 2014. Observation of mega-dune evaporation after various rain events in the hinterland of Badian Jaran desert. Chinese Science Bulletin, 59, 162–171. doi: 10.1007/s11434-013-0050-3.

Ma SH, Li ZL, Wang NA, Ning K, Li M. 2015. Mineralogical assemblage in surface sediments and its formation mechanism in the groundwater recharged lakes: A case study of lakes in the Badain Jaran Desert. Journal of Lake Sciences, 27(4), 727–734 (in Chinese with English abstract). doi: 10.18307/2015.0422.

McCormack J, Viehberg F, Akdemir D, Immenhauser A, Kwiecien O. 2019. Ostracods as ecological and isotopic indicators of lake water salinity changes: the Lake Van example. Biogeosciences, 16, 2095–2114. doi: 10.5194/bg-2018-476.

Michelson AV, Boush LP. 2017. A quantitative inference model for conductivity using non-marine ostracode assemblage on San Salvador Island, Bahamas: Paleosalinity records from two lakes. Palaeogeography, Palaeoclimatology, Palaeoecology, 477, 27–39. doi: 10.1016/j.palaeo.2017.04.002.

Mischke S, Almogi-Labin A, Ortal R, Rosenfeld A, Schwab MJ, Boomer I. 2010. Quantitative reconstruction of lake conductivity in the Quaternary of the Near East (Israel) using ostracods. Journal of Paleolimnology, 43, 667–688. doi: 10.1007/s10933-009-9359-y.

Mischke S, Herzschuh U, Massmann G, Zhang C. 2007. An ostracod-conductivity transfer function for Tibetan lakes. Journal of Paleolimnology, 38, 509–524. doi: 10.1007/s10933-006-9087-5.

Odum HT. 1951. Notes on the strontium content of sea water, celestite radiolaria, and strontium snail shells. Science, 114, 211–213. doi: 10.1126/science.114.2956.211.

Rucker JB, Valentine JW, 1961. Salinity response of trace element concentration in *Crassostrea virginica*. Nature, 190, 1099–1100. doi: 10.1038/1901099a0.

Sampei Y, Matsumoto E, Dettman DL, Tokuoka T, Abe O. 2005. Paleosalinity in a brackish lake during the Holocene based on stable oxygen and carbon isotopes of shell carbonate in Nakaumi Lagoon, southwest Japan. Palaeogeography, Palaeoclimatology, Palaeoecology, 224, 352–366. doi: 10.1016/j.palaeo.2005.04.020.

Shen J, Wang SM, Matsumoto R, Zhu YX. 2000. A preliminary study on palaeosalinity recovery in Daihai, Inner Mongolia. Science Bulletin, 45(17), 1885–1889. doi: 10.3321/j.issn:0023-074X.2000.17.017.

Song SH, Nie ZL, Geng XX, Shen X, Wang Z, Zhu PC. 2023. Response of runoff to climate change in the area of runoff yield in upstream Shiyang River Basin, Northwest China: A case study of the Xiying River. Journal of Groundwater Science and Engineering, 11(1), 89–96. doi: 10.26599/JGSE.2023.9280009.

Sun J, Hu WF, Wang NA, Zhao LQ, An R, Ning K, Zhang XH. 2018. Eddy covariance measurements of water vapor and energy flux over a lake in the Badain Jaran Desert, China. Journal of Arid Land, 10(4), 517–533. doi: 10.1007/s40333-018-0057-3.

Turich C, Freeman KH. 2011. Archaeal lipids record paleosalinity in hypersaline systems. Organic Geochemistry, 42, 1147–1157. doi: 10.1016/j.orggeochem.2011.06.002.

Van der Meeren T, Ito E, Verschuren D, Almendinger JE, Martens K. 2011. Valve chemistry of Limnocythere inopinata (Ostracoda) in a cold arid environments-implications for paleolimnological interpretation. Palaeogeography, Palaeoclimatology, Palaeoecology, 306, 116–126. doi: 10.1016/j.palaeo.2011.04.006.

Wang DC. 1980. Hydrogeology. Beijing: Geological Publishing House, 49–54.

Wang HL, Zhen MP. 2010. Preliminary study of the correlation between hydrochemistry and salinity of lakes in the Qinghai-Tibetan Plateau. Acta Geologica Sinica, 84(10), 1518–1522 (in Chinese with English abstract). doi: 10.1017/S0004972710001772.

Wang LJ, Wang Z, Jiang GL, Nie ZL, Shen JM, Song SH. 2024. Variations in evaporation from water surfaces along the margins of the Badain Jaran Desert over nearly 60 years and influencing factors. Journal of Groundwater Science and Engineering, 12(3), 253–263. doi: 10.26599/JGSE.2024.9280019.

Wang NA, Ning K, Li ZL, Wang YX, Jia P, Ma L. 2016. Holocene high lake-levels and pan-lake period on Badian Jaran Desert. Science China Earth Sciences, 59, 1–10. doi: 10.1007/s11430-016-5307-7.

Wang Z, Wang LJ, Shen JM, Nie ZL, Meng LQ, Cao L, Wei SB, Zeng XF. 2021. Groundwater characteristics and climate and ecological evolution in the Badain Jaran Desert in the southwest Mongolian Plateau. China Geology, 4, 421–432. doi: 10.31035/cg2021056.

Wang Z, Wang LJ, Shen JM, Nie ZL, Cao L, Meng LQ. 2024. Groundwater recharge via precipitation in the Badain Jaran Desert, China. Journal of Groundwater Science and Engineering, 12(1), 109–118. doi: 10.26599/JGSE.2024.9280009.

Williams WD. 1966. The relationship between salinity and Sr/Ca in the lake water. Marine and Freshwater Research, 17, 169–176. doi: 10.1071/MF9660169.

Wu D, Zhou AF, Zhang JW, Chen JH, Li GQ, Wang Q, Chen L, Madsen D, Abbott M, Cheng B, Chen FH. 2020. Temperature-induced dry climate in basins in the northeastern Tibetan Plateau during the early to middle Holocene. Quaternary Science Reviews, 237, 106311. doi: 10.1016/j.quascirev.2020.106311.

Wu Y, Wang NA, Zhao LQ, Zhang ZY, Chen L, Lu Y, Lv XN, Chang JL. 2014. Hydrochemical characteristics and recharge sources of Lake Nuoertu in the Badian Jaran Desert. Chinese Science Bulletin, 59, 886–895. doi: 10.1007/s11434-013-0102-8.

Xu XN, Wang Y, Shen J, Wang Y. 2012. Discussion on feasibility of paleosalinity reconstruction of Lake Qinghai water by variations in body length of Ostracod valves. Acta Sedimentologica Sinica, 30(6), 1072–1079 (in Chinese with English abstract).

Yang QC, Jochum KP, Stoll B, Weis U, Börner N, Schwalb A, Frenzel P, Scholz D, Doberschütz S, Haberzettl T, Gleixner G, Mäusbacher R, Zhu LP, Andreae MO. 2014. Trace element variability in single ostracod valves as a proxy for hydrochemical change in Nam Co, central Tibet, during the Holocene. Palaeogeography, Palaeoclimatology, Palaeoecology, 399, 225–235. doi: 10.1016/j.palaeo.2014.01.014.

Yang XP, Williams MAJ. 2003. The ion chemistry of lakes and late Holocene desiccation in the Badain Jaran Desert, Inner Mongolia, China. Catena, 51, 45–60. doi: 10.1016/S0341-8162(02)00088-7.

Yang XP. 2000. Discovery of calcareous cementation layers and their paleoclimatic implications in the Badain Jaran Desert. Quaternary Science, 20(3), 295–297 (in Chinese with English abstract). doi: 10.3321/j.issn:1001-7410.2000.03.010.

Yu C, Wu LJ, Zhang YL, Wang XY, Wang ZC, Zhang Z. 2022. Effect of groundwater on the ecological water environment of typical inland lakes in the Inner Mongolian Plateau. Journal of Groundwater Science and Engineering, 10(4), 353–366. doi: 10.19637/j.cnki.2305-7068.2022.04.004.

Yu LS, Liu HB, Wan F, Hu ZF, Luo HD, Zhang XW. 2021. Geochemical records of the sediments and their significance in Dongping Lake Area, the lower reach of Yellow River, North China. Journal of Groundwater Science and Engineering, 9(2), 140–151. doi: 10.19637/j.cnki.2305-7068.2021.02.006.

Zhai DY, Xiao JL, Zhou L, Wen RL, Chang ZG, Wang X, Jin XD, Pang QQ, Itoh S. 2011. Holocene East Asian monsoon variation inferred from species assemblage and shell chemistry of the ostracodes from Hulun Lake, Inner Mongolia. Quaternary Research, 75, 512–522. doi: 10.1016/j.yqres.2011.02.008.

Zhang EL, Jones R, Bedford A, Langdon P, Tang HQ. 2007. A chironomid-based salinity inference model from lakes on the Tibetan Plateau. Journal of Paleolimnology, 38, 477–491. doi: 10.1007/s10933-006-9080-z.

Zhang EL, Shen J, Wang SM, Yin Y, Zhu YX, Xia WL. 2004. Quantitative reconstruction of the paleosalinity at Qinghai Lake in the past 900 years. Chinese Science Bulletin, 49(7), 697–701. doi: 10.1360/03wd0334.

Zhang JW, Holmes JA, Chen FH, Qiang MR, Zhou AF, Chen S. 2009. An 850-year ostracod-shell trace-element record from Sugan Lake, northern Tibetan Plateau, China: Implications for interpreting the shell chemistry in high-Mg/Ca waters. Quaternary International, 194, 119–133. doi: 10.1016/j.quaint.2008.05.003.

Zhang PX, Zhao BZ, Qian GM, Li HJ, XU LM. 1994. The study of paleoclimatic parameter of Qinghai Lake since Holocene. Quaternary Sciences, 3, 225–2378 (in Chinese with English abstract).

Zhang XL, Luo X, Jiao JJ, Li HL, Lian EG, Yang SY, Kong FC, Kuang XX, Zuo JC. 2021. Hydrogeochemistry and fractionation of boron isotopes in the inter-dune aquifer system of Badian Jaran Desert, China. Journal of Hydrology, 595, 125984. doi: 10.1016/j.jhydrol.2021.125984.

Zhang HS, Cai WT, Guo F, Bian C, Liu FD, Zhang L, Liu JW, Zhao M. 2023. Microbial community composition and environmental response characteristics of typical brackish groundwater in the North China Plain. China Geology, 6(3), 383–394. doi: 10.31035/cg2022073.

Zhu JF, Wang NA, Chen HB, Dong CY, Zhang HA. 2010. Study on the boundary and the area of Badain Jaran Desert based on remote sensing imagery. Progress In Geography, 29(9), 1087–1094 (in Chinese with English abstract). doi: 10.3724/SP.J.1084.2010.00199.